Am J Cancer Res 2022;12(10):4584-4601
www.ajcr.us /ISSN:2156-6976/ajcr0143770

Original Article

Shikonin impedes type 2 ovarian cancer progression via FasL/caspase-8 and mir-874-3p/XIAP axis and prohibits the properties of stemness

Yu-Hsun Chang[1*], Yu-Jung Lin[4*], Chih-Yang Huang[4,5,6,7,8], Tomor Harnod[2], Dah-Ching Ding[3,9]

Departments of [1]Pediatrics, [2]Neurosurgery, [3]Obstetrics and Gynecology, Hualien Tzu Chi Hospital, Buddhist Tzu Chi Medical Foundation, Tzu Chi University, Hualien 970, Taiwan; [4]Cardiovascular and Mitochondrial Related Disease Research Center, Hualien Tzu Chi Hospital, Buddhist Tzu Chi Medical Foundation, Hualien 970, Taiwan; [5]Graduate Institute of Biomedical Sciences, China Medical University, Taichung 404, Taiwan; [6]Department of Medical Research, China Medical University Hospital, China Medical University, Taichung 404, Taiwan; [7]Department of Biological Science and Technology, Asia University, Taichung 404, Taiwan; [8]Center of General Education, Buddhist Tzu Chi Medical Foundation, Tzu Chi University of Science and Technology, Hualien 970, Taiwan; [9]Institute of Medical Sciences, Tzu Chi University, Hualien 970, Taiwan. [*]Equal contributors.

Received April 27, 2022; Accepted September 23, 2022; Epub October 15, 2022; Published October 30, 2022

Abstract: Ovarian cancer is the most lethal gynecological cancer in women. Shikonin (SHK), derived from *Lithospermum eryothrorhizon*, can reduce cancer activity; however, its clinical effect on type 2 ovarian cancer cells remains undetermined. Here, we studied the effects of SHK on type 2 ovarian cancer using the KURAMOCHI, OVSAHO, CP70, and ascites E04 cell lines. The proliferation curve and half-maximal inhibitory concentration of SHK for the cell lines were evaluated using the second-generation tetrazolium dye assay and the cell viability were determined by the annexin V/PI as well as TUNEL assay. The caspase dependent pathway was performed by western blotting assay with pan-caspase inhibitor Z-VAD-FMK and SHK induced miR-874-3p expression thus suppressed anti-apoptosis markers XIAP and Bcl-xL. The effect of SHK on type 2 ovarian cancer cell migration and invasion was evaluated using the wound healing and transwell assays. Quantitative RT-PCR and western blot was used to evaluate cancer stem cell (CSC)-related gene/protein (*OCT4, SOX2, NANOG, ALDH1*, and *C-MYC*) expressions, sphere formation assay was executed and a xenograft animal model for in vivo antitumor effects of SHK. Taken together, Shikonin suppressed type 2 ovarian cancer cell viability, migration, and invasion abilities; decreased CSC-related markers expression as well as the sphere colony numbers. It also reduced the tumorigenicity of KURAMOCHI ALDH+ cells and induced anti-tumor effect in a xenograft model. Thus, SHK could contribute a potential therapeutic strategy on type 2 ovarian cancer cells via multiple functions.

Keywords: Shikonin, type 2 ovarian cancer, apoptosis, miR-874-3p, metastasis, cancer stem cell

Introduction

Ovarian cancer is the second most prevalent gynecological cancer in Taiwan. It is currently the leading cause of female mortality in Taiwan and around the world [1, 2]. According to the Taiwan cancer registry, there are about 1000 new-onset ovarian cancer cases each year with a median onset age of 55 years.

Kurman et al. categorized ovarian cancer into type 1 and type 2 cell origins [3, 4], and the latter constitutes 85% of all ovarian cancers. Type 1 ovarian cancer shows a shared lineage with related benign cystic neoplasm, often through an intermediate (borderline tumor) step, which supports the morphological continuum of tumor progression from benign ones. However, Type 2 cells have a high level of genetic instability and are characterized by a TP53 mutation. Type 2 ovarian cancer is usually rapidly growing and highly aggressive, without well-defined precursor lesions, and is almost always diagnosed in the advanced stage. High-grade serous carcinomas (HGSC), carcinosarcomas, and undifferentiated carcinomas are regarded to be type 2 ovarian cancer. Moreover, it is typically asymptomatic in the early stage, although

with high histological malignancy [5] and more than two-thirds of the patients are diagnosed at later stages. This leads to an unsatisfactory prognosis, with 45.6% of the patients presenting with a 5-year survival rate [6]. The challenge to improve techniques for early diagnosis and treatment protocols for ovarian cancer is an urgent necessity for female public health in the 21st century.

Shikonin (SHK) is a naphthoquinone derived from the roots of the herbal plant *Lithospermum eryothrorhizon* and is used as an anti-inflammatory and anti-microbial agent in traditional Chinese medicine to treat burn wounds and sore throats [7, 8]. In recent years, SHK has been demonstrated to have anti-tumor effects-inducing liver cancer cell apoptosis, inhibiting melanoma proliferation, and killing leukemia cells [9-11]. In addition, SHK has been shown the cytotoxic effect on multi-drug-resistant cell lines and enhancement of chemotherapeutic sensitivity in various cancers. In colon cancer, SHK enhanced cisplatin-induced cell apoptosis; in glioblastoma, SHK synergistically kills tumor cells when combined with erlotinib; and in triple-negative breast cancer cells, SHK could induced cell cycle arrest [10, 12, 13]. Furthermore, SHK was reported to induce receptor-interacting protein 1 (RIPK1)-dependent necroptosis [14].

MiR-874 was first found in normal cervical tissue [15]. Several studies have shown that miR-874 suppressed various tumor proliferation and metastasis [16, 17]. MiR-874 could modulate epithelial ovarian cancer (EOC) cells apoptosis by directly regulating X-linked inhibitor of apoptosis protein (XIAP) expression in cisplatin-resistant EOC cells and sensitizing EOC cells to cisplatin through inhibit anti-apoptosis related protein [18].

A previous study showed that SHK-binding nanoparticles could kill ovcar-5 cells [19]. Another study revealed that it could kill SKOV-3 cells by inhibiting the phosphorylation of Src and FAK [20]. However, only type 1 ovarian cancer cell lines or non-ovarian cancer cell lines have been tested in these studies. The effects of the treatment on type 2 ovarian cancer have not been determined yet. Here, we reveal the cytotoxic effects of SHK on type 2 ovarian cancer using the KURAMOCHI, OVSAHO, CP70, and ascites E04 cell lines. We also determined the cellular mechanisms by which SHK succeed in destroying type 2 ovarian cancer cells and had an impact on CSC. Thus, the results illustrate a prospective drug in ovarian cancer.

Materials and methods

Cell culture

Four human ovarian cancer cell lines (KURAMOCHI, OVSAHO, CP70, and Ascites E04) were used in our study. The KURAMOCHI and OVSAHO cell lines were purchased from the Japan cell bank system. Both cell lines were matched with type 2 ovarian cancer characteristics [21]. They were maintained in RPMI 1640 (Sigma, St. Louis, MO) supplemented with 10% fetal bovine serum (FBS), 0.1% non-essential amino acids (NEAA), 2 mM L-glutamine, and 1% penicillin-streptomycin. The CP70 cell line is a cisplatin-resistant cell line [22]. It is maintained in RPMI 1640 (Sigma) supplemented with 5% FBS (Biological Industries, Kibbutz, Israel) and 10 mM HEPES (Sigma), 4 mM L-glutamine (Sigma), 1 mM sodium pyruvate (Sigma), 1 × non-essential amino acids (Sigma), 1% penicillin and streptomycin (Sigma). Ascites E04 cells were collected from a patient with stage 3C ovarian HGSC. After collection, the ascites cells were re-suspended after centrifugation at 1300 rpm. We collected the pellet and froze it at -80°C. After thawing, the cells were incubated with a medium that consisted of MCDB105/M199 (1:1, Sigma) supplemented with 10% FBS and 1% penicillin-streptomycin. All cells are incubated at 37°C with 5% CO_2.

Chemicals and antibodies

Shikonin was purchased from Sigma-Aldrich (St. Louis, MO, USA) and dissolved in DMSO (Sigma-Aldrich). Antibodies were obtained as follows: caspase 3 and 8, cleaved caspase 3 and 8 from Cell Signaling Technology (MA, USA); beta-actin and XIAP from Abcam (Cambridge, UK); Bcl-xL from Santa Cruz (Tx, USA); the goat IgG-HRP secondary antibodies against rabbit and mouse from Cell Signaling Technology (MA, USA), FITC and APC-conjugated secondary antibodies from Sigma (MO, USA).

Cell viability and cell death determination

The XTT assay (Biological Industries Ltd., Kibbutz Beit Haemek, Israel) and CCK-8 assay

(Dojindo Molecular Technologies) were used to detect cell viability following the manufacturer's instructions. Cells were seeded in 96-well plates and treated with the SHK. The XTT solutions and N-methyl dibenzopyrazine methyl sulfate (PMS) were defrosted in a 37°C bath immediately prior to use. The PMS is added to the XTT solution immediately before use. After 2-5 h of incubation at 37°C, the optical density (OD) of the wells was determined using a spectrophotometer (ELISA reader) at a wavelength of 450 nm and a reference wavelength of 650 nm. The CCK-8 solutions 10 μl were added to each well and incubated for 1 hour in the incubator, the OD of the wells at 450 nm were measured by microplate reader.

Then the IC50 of all four cell lines was obtained. The 4PL (four parameter logistic regression) method described in previous literature was used for counting IC50 [23]. The equation is expressed as follows: $Y = d + (a - d)/(1 + (X/c)^b)$; where Y = response, X = concentration, a = the bottom of the curve, d = the top of the curve, b = the slope factor, and c = the concentration corresponding to the response midway between a and d [24].

Annexin V/PI staining assay

Cells were cultured in the presence or absence of SHK under IC50. Apoptotic cells were examined using annexin V-FITC detection kits (BD Pharmingen™) according to the manufacturer's instructions. Cells were collected and treated with 5 μl of FITC Annexin V and 5 μl PI, then incubated for 15 minutes in the dark. After incubation, analyze the apoptosis by flow cytometry within 1 hour.

MiRNA mimics transfection

Cells were transfected with miR-874-3p mimics or inhibitors with negative control (50 nM) by Lipofectamine 2000 (Invitrogen) following the manufacturer's protocol.

Wound healing-migration assay

Cells were seeded in a six-well plate and grown until they reached 90-100% confluency. A scratch was made through the cell layer using a sterile micropipette tip. The cells were washed with phosphate buffer saline (PBS) and the complete medium was added with SHK or as control. Wounded areas were photographed under a light microscope at 4X objective at 0, 7, and 24 h. The wound area was calculated and compared with that at 0 h using percentage.

The different tumor cell lines (5×10^4 cells) were seeded into the top well of a 24-well transwell Boyden chamber with an 8 μm pore size (Costar, Corning Inc., Corning, NY, USA). After 48 h of migration, crystal violet (Sigma) was used to stain the migrated cells. The stained cells were counted using a bright-field microscope (Nikon, Tokyo, Japan).

Invasion assay

The Matrigel invasion assay was performed using Matrigel-coated Boyden chambers with 8 μM pore filter inserts in 24-well plates (BD) as previous study [25]. Briefly, 5×10^4 tumor cells of each cell line in 200 μl 5% FBS-supplemented culture medium were added to the inserts, followed by 500 μl 10% FBS-supplemented medium to the respective wells. Treatment with or without SHK (with IC50 for each kind of cell) was added to both upper as well as lower chambers. After 24 h, the non-invaded cells were gently removed with cotton swabs; invaded cells were first fixed in 4% formaldehyde and then stained with Giemsa, air-dried, counted, and photographed.

Quantitative real-time PCR

Gene expressions of CSC-related genes were assessed for *NANOG, SOX2, OCT4, C-MYC, ALDH1* and miR-874-3p. Glyceraldehyde 3-phosphate dehydrogenase (*GAPDH*) and U6 were used as an internal control. Table S1 lists the primer sequences used. In brief, real-time PCRs were performed by using FastStart Universal SYBR Green Master (ROX, Roche, Indianapolis, IN, USA) and a qPCR detection system (ABI Step One Plus system, Applied Biosystems, Foster City, CA, USA). Each target gene's expression levels were calculated as $2^{-\Delta\Delta Ct}$ [26]. Three readings for each experimental sample were obtained for each gene of interest. In addition, the experiments were repeated in triplicate.

Soft agar assay

Cells were suspended in RPMI 1640 containing 0.4% agar, 10% fetal bovine serum, 1% penicil-

lin-streptomycin and seeded on RPMI containing 0.8% agar, 10% fetal bovine serum and 1% penicillin-streptomycin. Colonies < or > 50 μm were photographed and counted at day 21. All the experiments were performed in triplicate wells for three times.

The TUNEL assay

A TUNEL Assay Kit (Roche, IN, USA) was used to detect the apoptosis of cells and xenografts according to the manufacturer's protocols and previous described [27]. Cells and tumor sections were fixed using 4% paraformaldehyde and treated with the TUNEL assay kit. The DNA strand breaks were identified by TUNEL probes.

Western blot

Whole cells were suspended in Laemmli Buffer (Bio-Rad Laboratory, USA). Protein concentrations were measured using the BCA Protein Assay Kit (Pierce, USA). Equal amounts of protein were separated using Sodium Dodecyl Sulphate-Polyacrylamide Gel Electrophoresis (SDS-PAGE) and transferred to a polyvinylidene difluoride (PVDF) membrane (Bio-Rad Laboratory, USA). The membrane was incubated with the primary antibodies (1:200, caspase 3, 8) overnight at 4°C and then with secondary antibodies (1:5000 diluted anti-rabbit immunoglobulin G horseradish peroxidase (HRP) for staining (Amersham GE, Taipei, Taiwan, China). The HRP signals were detected using an electrochemiluminescence kit (Promega, Fitchburg, WI, USA).

Xenograft experiment

The procedures for animal experiments were carried out in adherence to the National Institutes Health Guide for the Care and Use of Laboratory Animals and approved by the Animal Research and Care Committee of the Buddhist Tzu Chi General Hospital (106-20). The NOD-SCID (strain name: NOD.CB17-Prkdcscid/JTcu) mice were obtained from Tzu Chi University. The KURAMOCHI ALDH+ cells (1×10^6) were injected subcutaneously into the backs of 4-5-week-old female NOD-SCID mice. After tumors reached 50 mm^3 in size, the control group was injected with the vehicle (10% DMSO in PBS) and the treatment group was injected with SHK (1 mg/kg) on alternate days for 2 wks. Tumor dimensions (length and width) were measured using a caliper. Tumor volumes are calculated by the formula V [volume] = 1/2 (L [length] × W [width]^2).

For histological examination, the xenograft tumor tissues were fixed in 4% paraformaldehyde. We cut 6-μm-thick paraffin-embedded tumor sections and stained these with hematoxylin and eosin. Tumor tissue was assessed at × 200 total magnification. Cell density and morphology were then determined.

Statistical analysis

Values are presented as the mean ± SD for at least three independent experiments. Statistical comparisons were analyzed using one-way ANOVA followed by Tukey's post-hoc with GraphPad Prism 6 (La Jolla, CA, USA). $P < 0.05$ indicates a significant difference.

Results

Low concentration of SHK induces apoptosis in type 2 ovarian cancer cells

We evaluated the proliferation curve and half-maximal inhibitory concentration (IC50) of SHK on ovarian cancer cells (KURAMOCHI, OVSAHO, CP70, and ascites-derived cancer cells [E04]). The KURAMOCHI and CP70 cells exhibited a normal growth curve (Figure S1), whereas OVSAHO and E04 cells showed slower growth than KURAMOCHI and CP70 cells. The IC50 of SHK for KURAMOCHI (0.507 μM), OVSAHO (0.9165 μM), CP70 (0.258 μM), ascites E04 (1.338 μM) and NOV cells (0.183 μM) after 24 h of treatment are shown in **Figure 1**. We then evaluated the apoptosis status of the KURAMOCHI, OVSAHO, CP70 and ascites E04 cells after SHK treatment using the terminal deoxynucleotidyl transferase dUTP nick end labeling (TUNEL) assay to detect DNA fragmentation. There were more than 30% apoptotic cells in SHK-treated ovarian cancer cells and less than 5% in the DMSO-control (**Figure 2A-D**). Next, we utilized the Annexin V/PI assay to examine the populations of apoptotic cell after SHK treatment. The FACS analysis confirmed that SHK increased the percentages of apoptotic cell in KURAMOCHI (35.7%), OVSAHO (45.4%), CP70 (37.5%) and ascites E04 cells (33.2%) compare to control (**Figure 2E-I**).

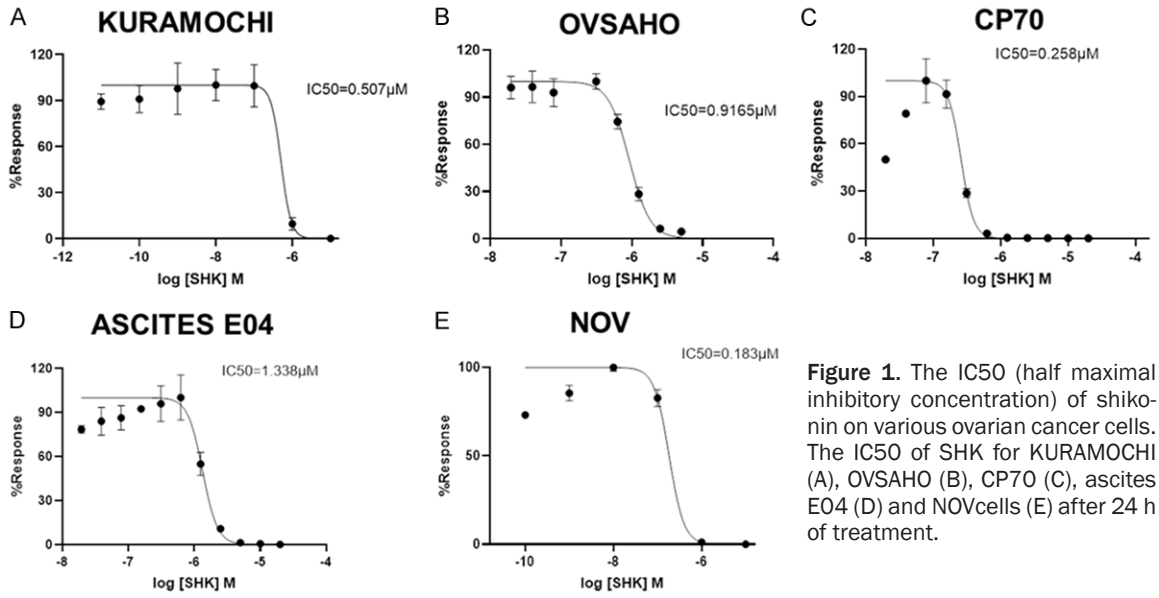

Figure 1. The IC50 (half maximal inhibitory concentration) of shikonin on various ovarian cancer cells. The IC50 of SHK for KURAMOCHI (A), OVSAHO (B), CP70 (C), ascites E04 (D) and NOVcells (E) after 24 h of treatment.

Shikonin activates FasL/caspase-8 signaling pathway and inhibited by pan-caspase inhibitor Z-VAD-FMK pretreatment

To investigate whether the cytotoxic properties of SHK were caused by apoptosis pathway, the protein expression of apoptosis was investigated. Protein levels of FasL, cleaved caspase 8, caspase 3, and caspase 7 were increased in SHK-treated KURAMOCHI (**Figure 3A**), OVSAHO (**Figure 3B**), CP70 (**Figure 3C**) and ascites E04 cells (**Figure 3D**). Thus, our results show that SHK induces apoptosis through FasL/caspase-8 signaling pathway. Moreover, we pretreated the pan-caspase inhibitor Z-VAD-FMK with ovarian cancer cells before SHK and found the cytotoxic effects were inhibited by CCK-8 assay (**Figure 4A-D**). Z-VAD-FMK also blocked caspase-8 and caspase-3 induction by SHK in KURAMOCHI (**Figure 4E**) and OVSAHO cells (**Figure 4F**).

Shikonin induces apoptosis by modulating miR-874-3p/XIAP axis in type 2 ovarian cancer cells

To explore the mechanism to induce ovarian cancer apoptosis by SHK, we explored and examined miR-874-3p, miR-125b-5p [28] and miR-4782-3p [29] (data not shown) as tumor suppressor in ovarian cancer to see whether they could be induced by Shikonin in type 2 ovarian cancer cell and found the expression of miR-874-3p was increased after SHK treatment (**Figure 5A**, **5B**). Next, we transfected the mimic miR-874-3p and found it could induce KURAMOCHI and OVSAHO cell apoptosis (**Figure 5C-E**). However, knockdown of miR-874-3p reversed KURAMOCHI and OVSAHO cell apoptosis (**Figure 5F**, **5G**). Western blot assay showed that SHK and mimic 874-3p suppressed anti-apoptosis related protein XIAP and Bcl-xL (**Figure 5H**). Knockdown of miR-874-3p reversed the SHK effect on XIAP expression (**Figure 5I**), suggested that SHK might induce apoptosis through miR-874-3p/XIAP pathway as well in type 2 ovarian cancer cells.

Shikonin inhibits the wound healing capability of type 2 ovarian cancer cells

We used the wound healing assay to evaluate the migration capability of ovarian cancer cells with or without SHK treatment. Photographs of scratch areas at 0, 7, and 24 h after treatment are illustrated in **Figure 6**. In the KURAMOCHI cells, SHK significantly inhibited cell migration at 7 h (**Figure 6A**). However, at 24 h, the area was approximately closed. In OVSAHO (**Figure 6B**), the migration ability was slow. At 24 h, SHK-treated cells did not migrate and the area became larger than that at 0 h and 7 h. The OVSAHO cells might die during SHK treatment. In CP70 (**Figure 6C**) and ascites E04 cells (**Figure 6D**), SHK treatment significantly inhibit cell migration at 7 or 24 h. Taken together, SHK could inhibit cell migration in the wound healing experiment.

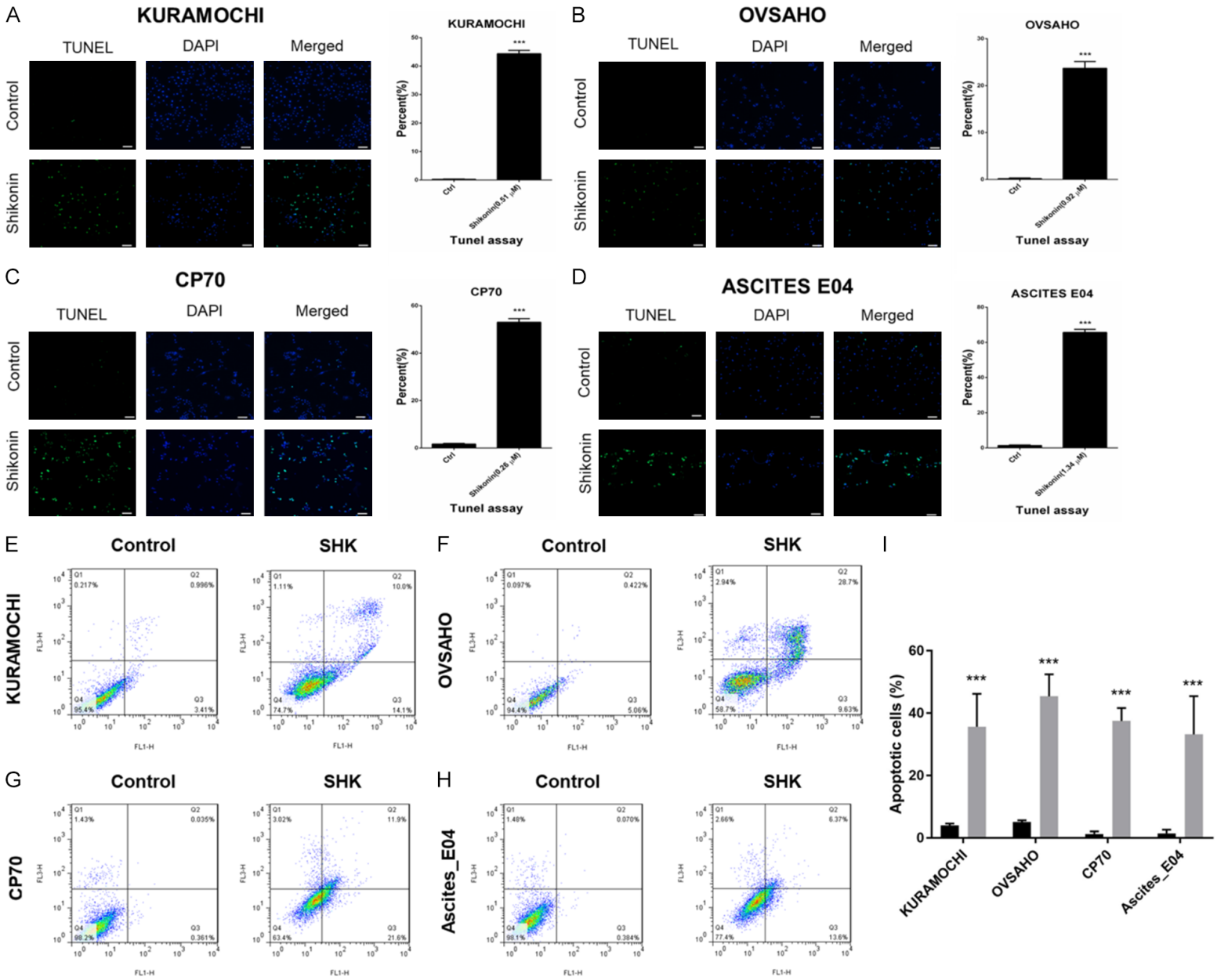
A
KURAMOCHI
TUNEL
DAPI
Merged
Control
Shikonin
KURAMOCHI
Percent(%)
Ctrl
Shikonin(0.51 μM)
Tunel assay
B
OVSAHO
TUNEL
DAPI
Merged
Control
Shikonin
OVSAHO
Percent(%)
Ctrl
Shikonin(0.92 μM)
Tunel assay
C
CP70
TUNEL
DAPI
Merged
Control
Shikonin
CP70
Percent(%)
Ctrl
Shikonin(0.26 μM)
Tunel assay
D
ASCITES E04
TUNEL
DAPI
Merged
Control
Shikonin
ASCITES E04
Percent(%)
Ctrl
Shikonin(1.34 μM)
Tunel assay
E
Control
SHK
KURAMOCHI
F
Control
SHK
OVSAHO
I
Apoptotic cells (%)
KURAMOCHI
OVSAHO
CP70
Ascites_E04
G
Control
SHK
CP70
H
Control
SHK
Ascites_E04

Figure 2. The terminal deoxynucleotidyl transferase dUTP nick end labeling (TUNEL) assay of various ovarian cancer cells. (A) Pictures and quantification of KURAMOCHI cell with or without SHK treatment for 24 h labeled with TUNEL assay and corresponding DAPI staining. Scale bar = 100 μm. (B) Pictures and quantification of OVSAHO cells incubated with SHK or without for 24 h labeled with TUNEL assay and corresponding DAPI staining. Scale bar = 100 μm. (C) Pictures and quantification of CP70 cells incubated with SHK or without for 24 h labeled with TUNEL assay and corresponding DAPI staining. Scale bar = 100 μm. (D) Pictures and quantification of Ascites_E04 cells incubated with SHK or without for 24 h labeled with TUNEL assay and corresponding DAPI staining. Scale bar = 100 μm. (E-H) Cancer cells were stained with Annexin V-FITC and PI after SHK treatment and performed by flow cytometry. (I) Percentages of apoptotic cells in (E-H) were quantified. The experiments were carried out in triplicate. ***P < 0.001.

Shikonin inhibits the migration and invasion abilities of type 2 ovarian cancer cells

We used the transwell assay to study the role of SHK on the migration and invasion abilities of various ovarian cancer cells. Photographs of migrating cells at 48 h after treatment are illustrated in **Figure 6**. It showed that the number of migrating cells decreased by 80% in different cell lines (**Figure 6E-H**). Photographs of invading cells from the 24 h are illustrated in **Figure 6E-H**. It showed that the number of invading cells decreased in different cell lines. Thus, SHK could inhibit type 2 ovarian cancer cell migration and invasion.

Type 2 ovarian cancer cells express the ALDH- cancer stem cell (CSC) marker

The CSC marker (ALDH) expression of various cancer cells was measured through flow cytometry using the Aldefluror assay. The percentage of the ALDH+ population in KURAMOCHI, CP70, E04, and OVSAHO cells was 2.2, 2.3, 0.8, and 8.6%, respectively (Figure S2). The ovarian CSC consisted of a small population of cancer cells.

Shikonin decreases the expression of CSC-related markers and suppresses stemness

We then used *quantitative real-time*-PCR (qPCR) to evaluate the effect of SHK on the expression of stem cell-related genes of type 2 ovarian cancer cells. The expression of CSC-related genes (*NANOG, OCT4, SOX2,* and *ALDH1*) was down-regulated in KURAMOCHI cells after treatment with SHK for 24 h (**Figure 7A**). In OVSAHO, CP70, and ascites E04 cells, all tested stem cell-related genes were down-regulated (**Figure 7B-D**). The protein expression of ALDH1 and SOX2 were also decreased under SHK treatment in different cell lines (**Figure 7E**, **7F**). The Soft agar assay showed that SHK could reduce the ability of sphere colony formation (**Figure 7G-J**). SHK significantly suppressed the numbers of colonies which diameter were > 50 μm in KURAMOCHI (**Figure 7G**) and CP70 cells (**Figure 7H**), decreased the diameter < 50 μm in OVSAHO and E04, (**Figure 7I**, **7J**). Taken together, SHK exhibited the capability to inhibit the property of cancer stemness in type 2 ovarian cancer.

Shikonin inhibited xenograft tumor growth via apoptosis

To evaluate the therapeutic potential of SHK on ovarian cells in vivo, we used the NOD-SCID mouse model to test the xenograft formation capability of type 2 ovarian CSC (KURAMOCHI ALDH+ cells). Treatment with SHK (1 mg/kg) significantly inhibited KURAMOCHI ALDH+ cells' tumor growth compared to the control group (**Figure 8A**). After 14 d of treatment, the tumor volume was reduced by 60% in the treatment group compared with the control group ($P < 0.05$). Further, the tumor tissues were performed by histological examination and histochemistry to determine the morphology and apoptosis of the cells. In the control group, the nuclei were large and irregular as compared to the SHK-treated group (**Figure 8B**). More cell death was also noted in SHK-treated tumors. There were significantly more TUNEL-positive cells in the tumor tissues of the SHK-treated group than the control ($P < 0.001$, **Figure 8C** and **8D**). These results indicated that SHK could inhibit in vivo tumor growth and kill tumor cells by inducing cell apoptosis.

Discussion

In this study we investigated the anti-type 2 ovarian cancer effects of SHK, a naturally occurring compound derived from *Lithospermum erythrorhizon*.

As ovarian cancer is the most lethal gynecological cancer, early detection and development of newly effective therapies to reduce mortality

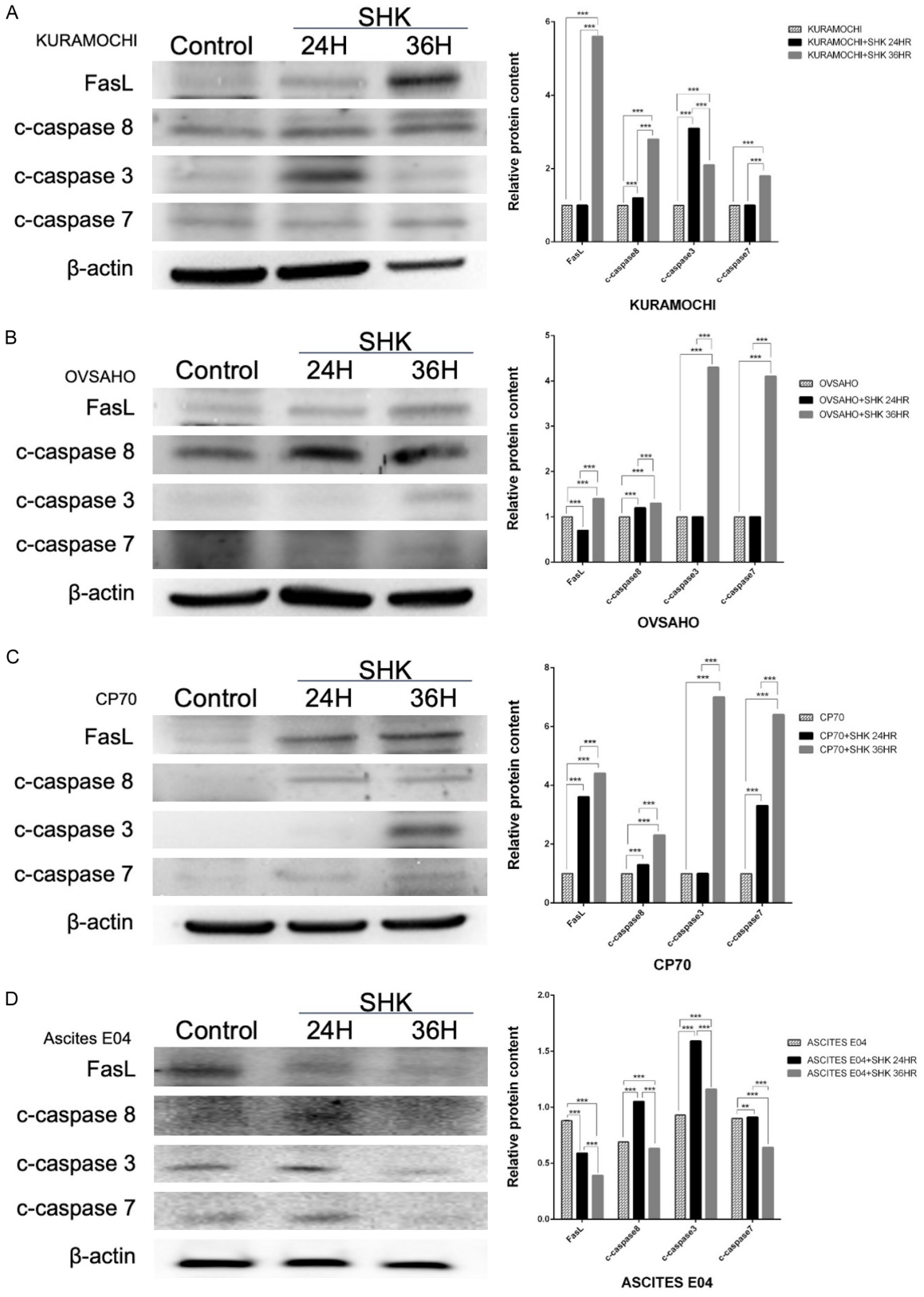

Figure 3. Shikonin activated the FasL/caspase-8 signaling pathway. Protein levels of FasL, cleaved caspase 3, caspase 8 were increased in SHK-treated various ovarian cancer cells. (A) KURAMOCHI and (B) OVSAHO (C) CP70 and (D) Ascites_E04 cells were treated with DMSO or SHK for indicated time intervals and western blot for FasL, cleaved caspase 3 and caspase 8 was performed. The experiments were carried out in triplicate. **P < 0.01, ***P < 0.001.

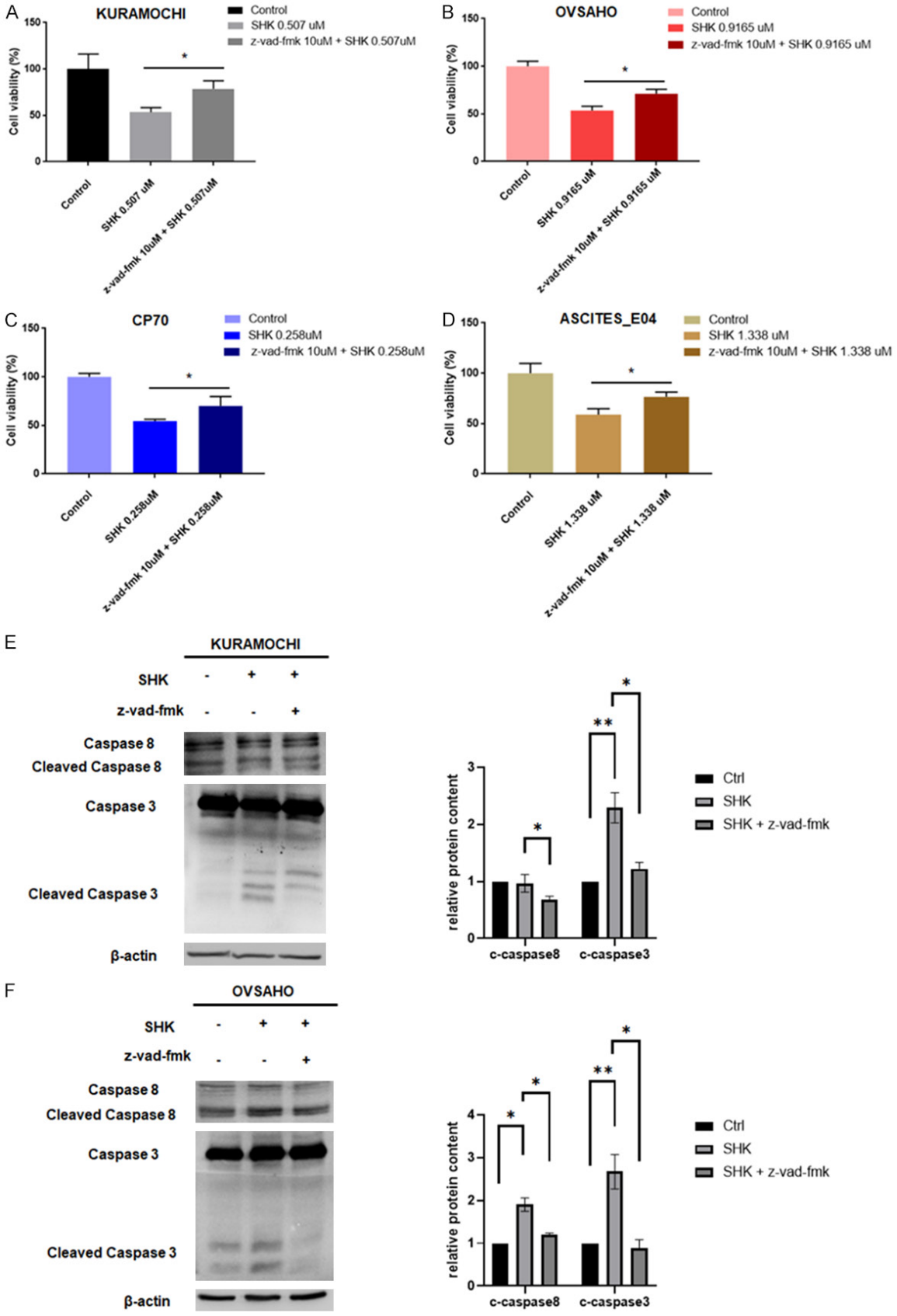
A
KURAMOCHI
Control
SHK 0.507 uM
z-vad-fmk 10uM + SHK 0.507uM
Cell viability (%)
B
OVSAHO
Control
SHK 0.9165 uM
z-vad-fmk 10uM + SHK 0.9165 uM
C
CP70
Control
SHK 0.258uM
z-vad-fmk 10uM + SHK 0.258uM
D
ASCITES_E04
Control
SHK 1.338 uM
z-vad-fmk 10uM + SHK 1.338 uM
E
KURAMOCHI
SHK
z-vad-fmk
Caspase 8
Cleaved Caspase 8
Caspase 3
Cleaved Caspase 3
β-actin
relative protein content
c-caspase8
c-caspase3
Ctrl
SHK
SHK + z-vad-fmk
F
OVSAHO

Figure 4. Effects of pan-caspase inhibitor Z-VAD-FMK on SHK induced cell apoptosis. (A) KURAMOCHI and (B) OVSAHO (C) CP70 and (D) Ascites_E04 cells were pretreated with Z-VAD-FMK 10 μM for 4 h then treated with indicated IC50 of SHK and examined by CCK-8 assay. The protein level of cleaved caspase 3 and caspase 8 in (E) KURAMOCHI and (F) OVSAHO were detected by western blot after pre-treated Z-VAD-FMK 10 μM and SHK treatment. The experiments were carried out in triplicate. *P < 0.05, **P < 0.01.

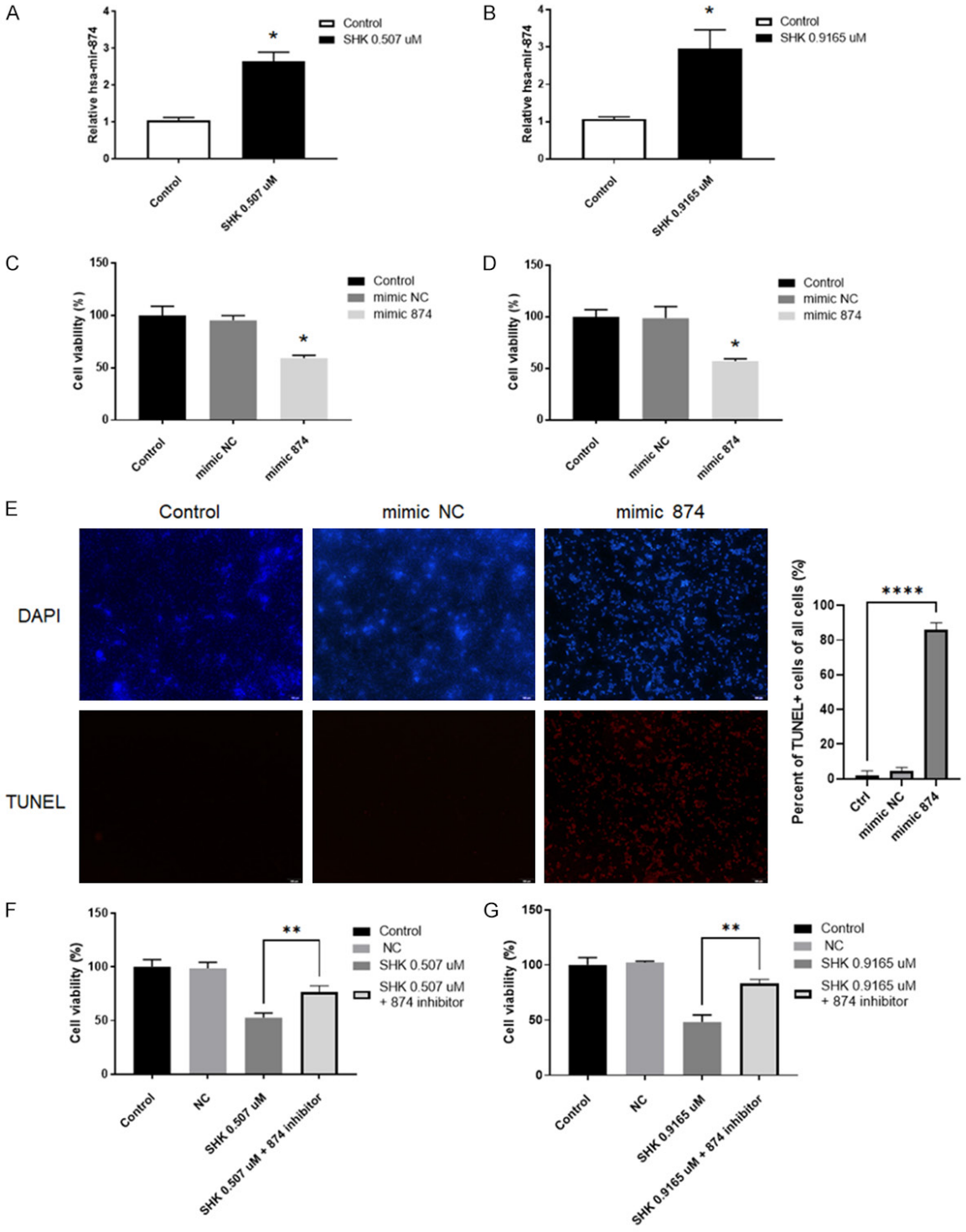

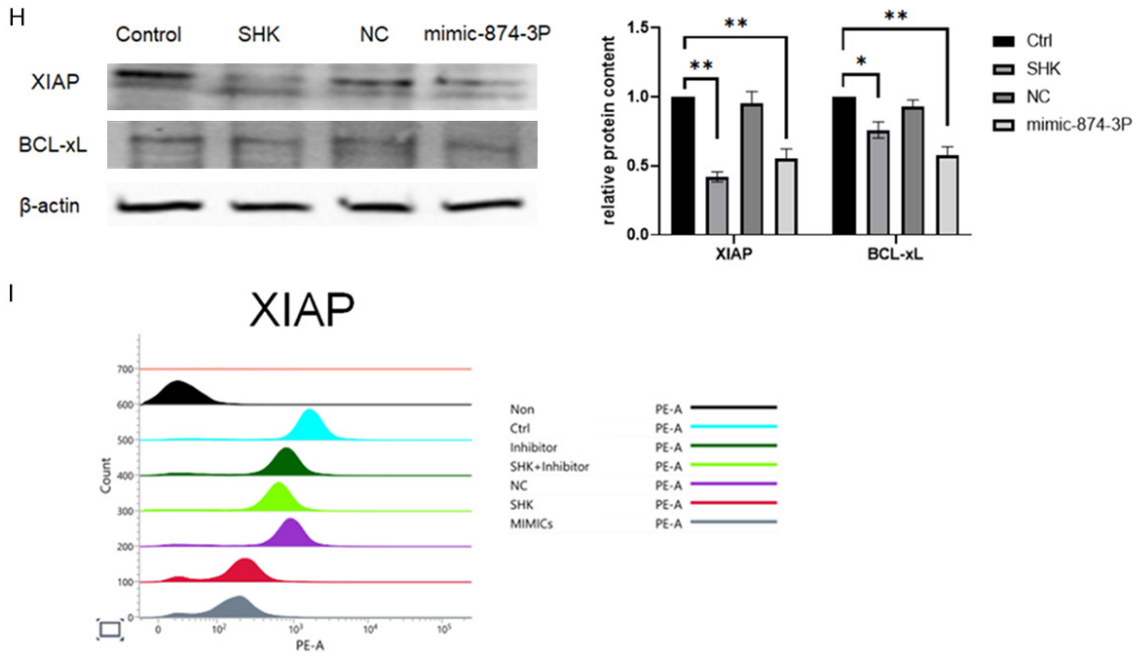

Figure 5. Shikonin induce ovarian cancer cells apoptosis by inducing miR-874-3p/XIAP pathway. MiR-874-3p expression was up-regulated by SHK in (A) KURAMOCHI and (B) OVSAHO cells. Transfected with 50 nM mimic miR-874 suppressed cell viability in (C) KURAMOCHI and (D) OVSAHO cells. (E) TUNEL assay showed the apoptotic KURAMOCHI cells after transfected 50 nM mimic miR-874. Knockdown of miR-874-3p reversed the cell viability in (F) KURAMOCHI and (G) OVSAHO cells. (H) Protein levels of XIAP and Bcl-xL were decreased in SHK-treated and 50 nM mimic miR-874-3p KURAMOCHI cells. (I) Protein levels of XIAP were restored by miR-874-3p inhibitor under SHK treatment in KURAMOCHI cells. *P < 0.05.

are necessary. However, even the origin and pathogenesis of epithelial ovarian cancers remained unclear so far. Despite many studies that have scrutinized the ovaries for precursor lesions, no definite conclusions have been found. Recently, the fallopian tube epithelia were thought to be the cells of origin for type 2 ovarian cancer, which subsequently metastasize to the ovary [5, 20]. This may explain why such tumors have not been detected at early stages as detection efforts have been focused on the ovary itself. Further studies have revealed that the putative precursors of serous carcinoma in women with BRCA mutations are usually present in the fimbriated end of the fallopian tube [30], and HGSC evidenced DNA damage and p53 mutations that have arisen from the fallopian tube epithelium [31]. It has been shown that epithelial ovarian cancer is not a single disease but an amalgamation of a diverse group of tumor cells that can be distinguished by their distinctive morphologic and molecular genetic features. Therefore, predictably, the current treatments against type 1 cells cannot provide ideal results for most ovarian cancers.

The current standard first-line therapy for ovarian HGSC is a combination of cytoreductive surgery and tri-weekly carboplatin/paclitaxel-based chemotherapy [32]. More than 50% of the patients may achieve a temporary complete remission through this regimen. However, a majority of the patients develop recurrent cancer within the first 2 years, with only 10-30% of them achieving long-term survival [33]. Recently, a polyp (ADP-ribose) polymerase inhibitor (PARPi) has been approved for the treatment of ovarian cancer patients who fail three or more lines of chemotherapy and have a germline mutation of BRCA1/2 [34].

In view of no new guidelines for the treatment of ovarian cancer in recent years, we designed this study to test the effects of SHK on type 2 ovarian cancer cells by using primary cell lines from patient-derived xenografts [35, 36]. We found that the pure compound SHK can effectively kill type 2 ovarian cancer cells by activating apoptosis in vitro and in vivo. Several human ovarian cancer cell lines (KURAMOCHI, OVSAHO, CP70, and ascites E04 cells collected from a Taiwanese patient with ovarian cancer)

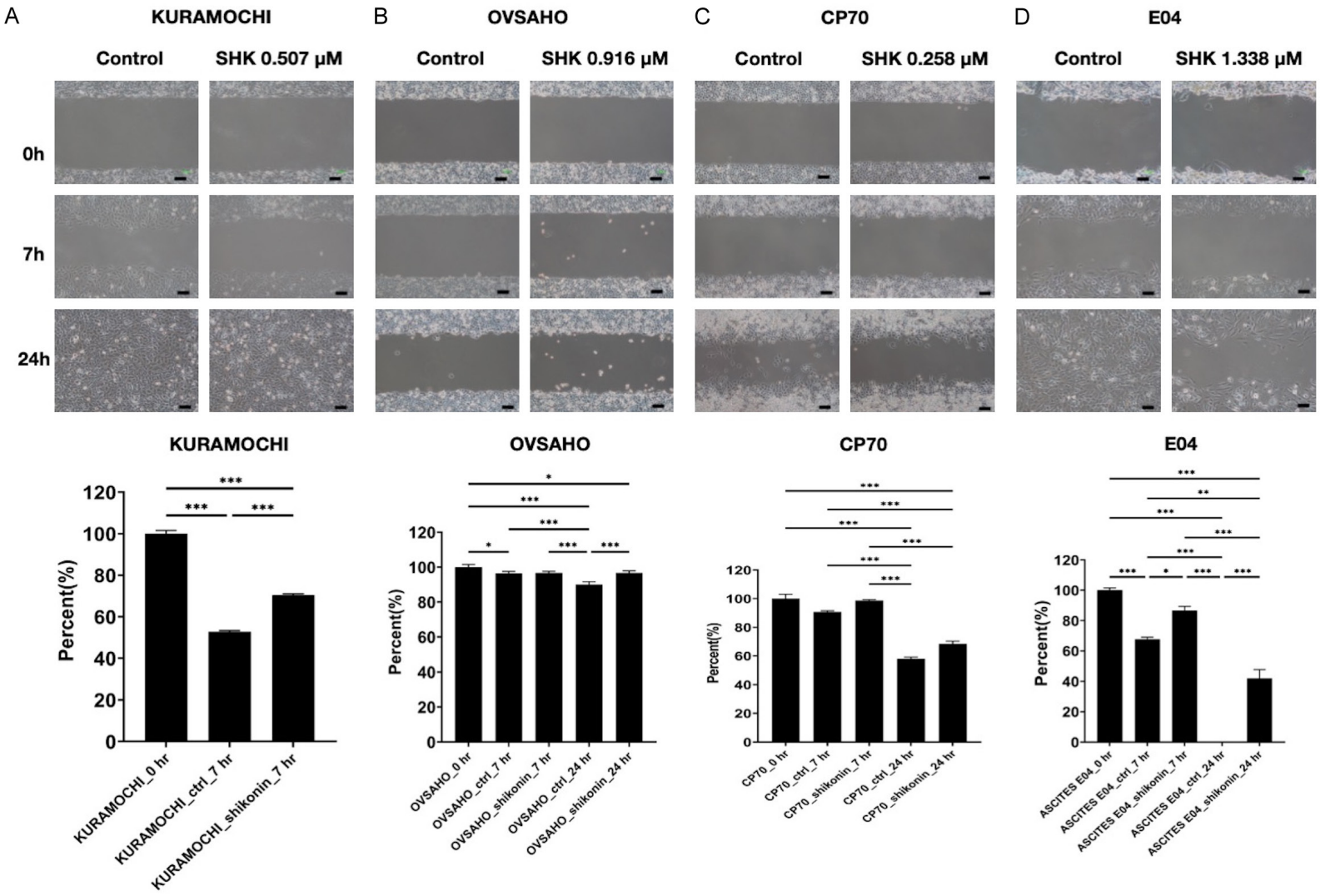
A
KURAMOCHI
Control
SHK 0.507 μM
B
OVSAHO
Control
SHK 0.916 μM
C
CP70
Control
SHK 0.258 μM
D
E04
Control
SHK 1.338 μM
0h
7h
24h
KURAMOCHI
Percent(%)
KURAMOCHI_0 hr
KURAMOCHI_ctrl_7 hr
KURAMOCHI_shikonin_7 hr
OVSAHO
OVSAHO_0 hr
OVSAHO_ctrl_7 hr
OVSAHO_shikonin_7 hr
OVSAHO_ctrl_24 hr
OVSAHO_shikonin_24 hr
CP70
CP70_0 hr
CP70_ctrl_7 hr
CP70_shikonin_7 hr
CP70_ctrl_24 hr
CP70_shikonin_24 hr
E04
ASCITES E04_0 hr
ASCITES E04_ctrl_7 hr
ASCITES E04_shikonin_7 hr
ASCITES E04_ctrl_24 hr
ASCITES E04_shikonin_24 hr

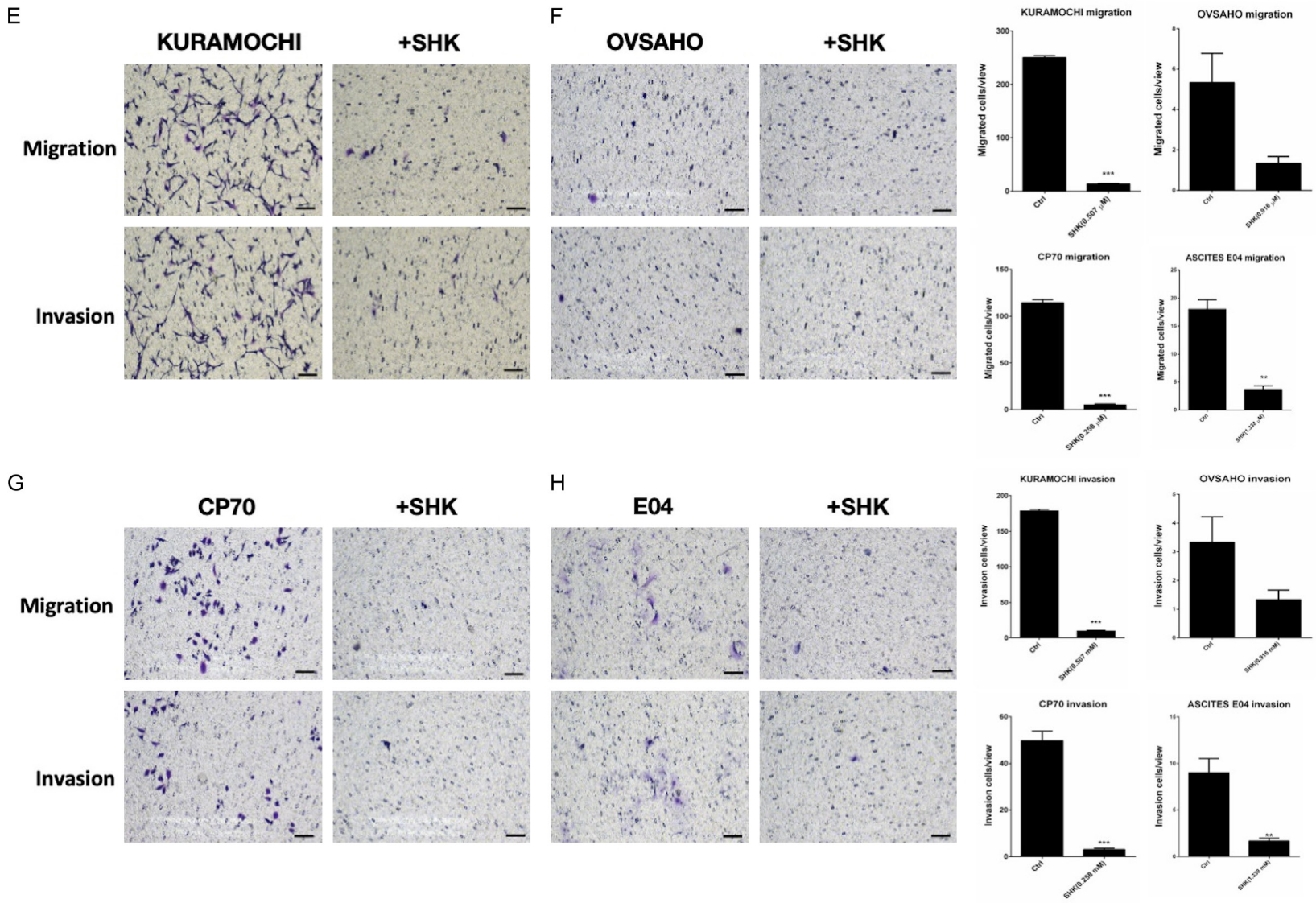

Figure 6. Shikonin inhibited ovarian cancer cells (KURAMOCHI, CP70, ascites E04, and OVSAHO) wound healing, migration and invasion capability. (A-D) The wound healing capability of various ovarian cancer cells with or without SHK treatment was photographed at 0, 7, and 24 h. (E-H) Transwell migration and invasion of ovarian cancer cells (KURAMOCHI, OVSAHO, CP70, and ascites E04) with shikonin (SHK) or without. After 48 h, migrated cells were stained with crystal violet and counted by bright-field microscope. The experiment was performed in triplicate. After 24 h, the non-invaded cells were gently removed with cotton swabs; invaded cells were fixed in 4% formaldehyde and then stained with Giemsa, air-dried, counted, and photographed. The experiment was performed in triplicate. *P < 0.05, **P < 0.01, ***P < 0.001.

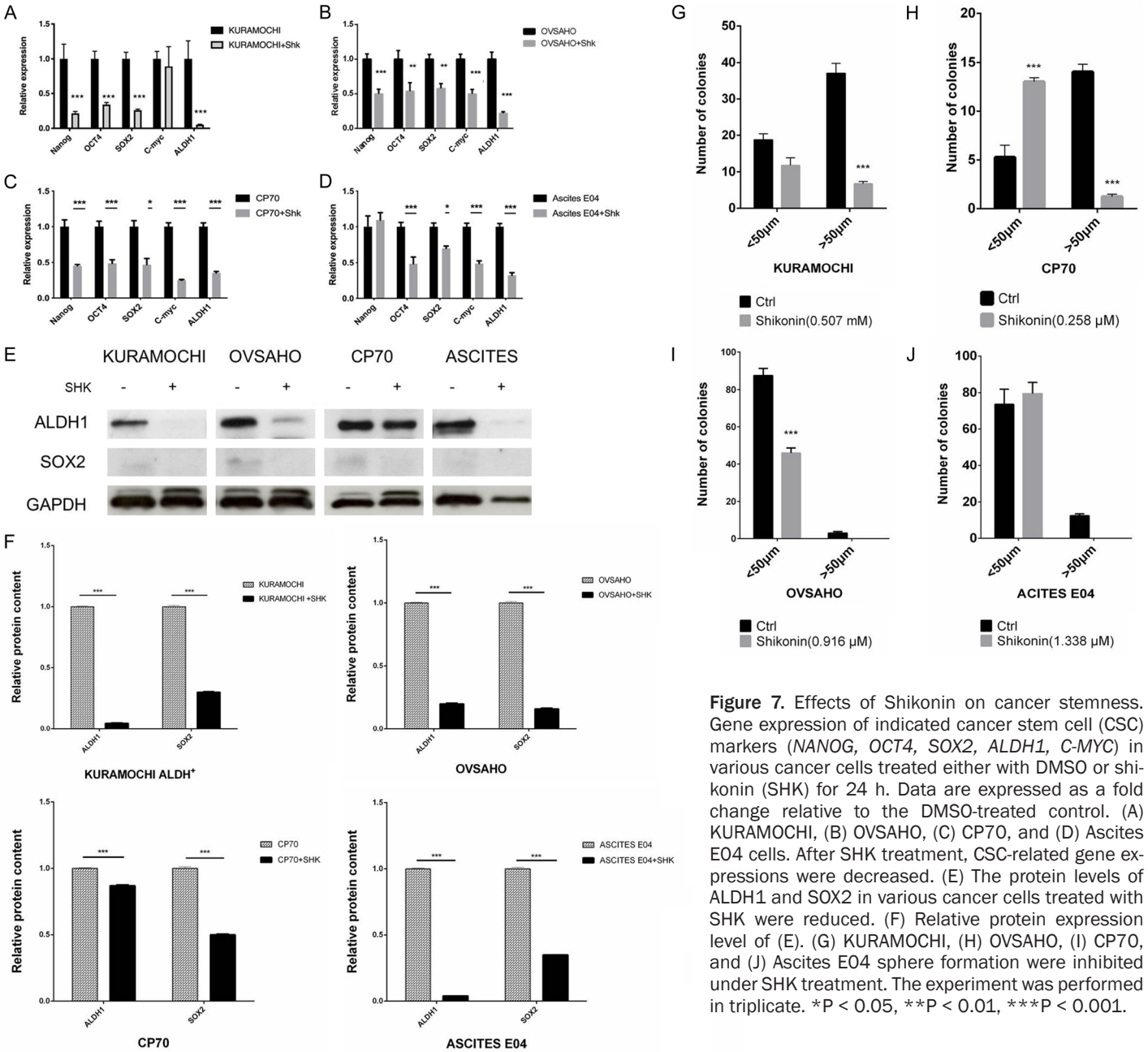

Figure 7. Effects of Shikonin on cancer stemness. Gene expression of indicated cancer stem cell (CSC) markers (*NANOG, OCT4, SOX2, ALDH1, C-MYC*) in various cancer cells treated either with DMSO or shikonin (SHK) for 24 h. Data are expressed as a fold change relative to the DMSO-treated control. (A) KURAMOCHI, (B) OVSAHO, (C) CP70, and (D) Ascites E04 cells. After SHK treatment, CSC-related gene expressions were decreased. (E) The protein levels of ALDH1 and SOX2 in various cancer cells treated with SHK were reduced. (F) Relative protein expression level of (E). (G) KURAMOCHI, (H) OVSAHO, (I) CP70, and (J) Ascites E04 sphere formation were inhibited under SHK treatment. The experiment was performed in triplicate. *P < 0.05, **P < 0.01, ***P < 0.001.

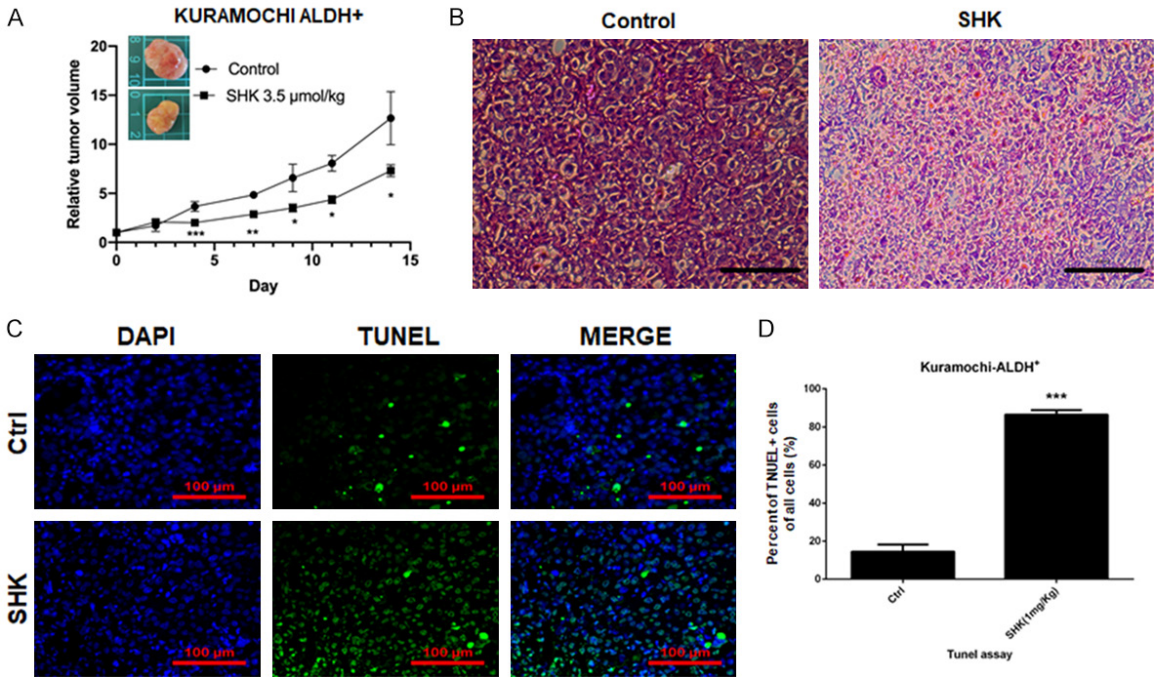

Figure 8. Shikonin (SHK) inhibited xenograft tumor growth via apoptosis. (A) SHK (3.5 μmol/kg) inhibited KURAMOCHI ALDH+ cells tumor growth. Tumor growth curves were illustrated for 14 d. Tumors grew slowly after SHK treatment. *P < 0.05, **P < 0.01, ***P < 0.001. (B) Hematoxylin and eosin staining of tumor tissue with SHK or without. Scale bar = 100 μm. (C) TUNEL assay of tumor tissue with SHK or without. Scale bar = 100 μm. (D) Quantification of TUNEL+ cells in both SHK and control groups. ***P < 0.001. After SHK treatment, there were significantly more apoptotic cells noted than those in controls.

were tested in this study. Cancer cell lines are currently used commonly in oncological experiments in the laboratory to find possible new treatments. The OVSAHO and KURAMOCHI cell lines have been documented in their higher genomic fidelity of TCGA [21], similar to type 2 ovarian cancer cells. In this study, we could find promising treatment effects of SHK on all four ovarian cancer cell lines. The importance of the study is that type 2 ovarian cancer (HGSC) constitutes 85% of all ovarian cancers and our results have explored the possibility of SHK as a treatment for ovarian cancer by evaluating its killing effects on type 2 ovarian cancer cells.

A previous study showed that SHK could decrease CSC-related gene expression in breast cancer cells [37]. The CSC theory supposes that stem cells can undergo self-renewal and are responsible for tumor initiation [38]. In ovarian cancer, CSCs are responsible for tumor initiation, progression, metastasis, and chemoresistance [38]. Therefore, therapy targeting CSC is needed for eliminating the unwanted CSC population. Ovarian CSC markers include embryonic stem cell markers (OCT4, SOX2, NANOG), ALDH1, and C-MYC [38]. In our study, we showed that SHK was effective in decreasing the expression of these ovarian CSC markers.

Apoptosis is a highly regulated and controlled process. Internal environmental stability is necessarily maintained by apoptosis which removes infected cells [39, 40]. Extreme apoptosis may result in autoimmune diseases [41], and less apoptosis may cause uncontrolled cell proliferation and tumor formation [42]. Two pathways of apoptosis have been documented with the extrinsic and intrinsic pathways, and both of them eventually activate caspase cascade to induce cell death [43]. Many chemotherapeutic drugs have been proved to induce apoptosis of tumor cells to achieve anti-tumor effects, and the drug resistance often occurs with escape of caspase [44]. Thus, inducing tumor cell apoptosis shows huge benefits in anti-tumor therapy and our results from a TUNEL assay have effectively shown the apoptosis of type 2 cells after SHK treatment by the

activation of caspase 3 and 8, and p53. Here, up-regulation of miR-874-3p by SHK was found in type 2 ovarian cancer. As previous studies showed, miR-874-3p plays an important role to suppress cancer cell viability and migration. We also elucidated that miR-874-3p could promote type 2 ovarian cancer cell apoptosis and inhibit XIAP protein expression as well. These results are in line with the previous finding in EOC and reveal that SHK might cause type 2 ovarian cancer cell death and inhibit migration via miR-874-3p/XIAP axis.

Moreover, reactive oxygen species (ROS) are formed naturally and act like two-edged swords in maintaining homeostasis of cells. Intracellular accumulation of ROS is another common mechanism through which chemodrugs and radiotherapeutic agents kill cancer cells [45]. Shikonin has been proved to induce ROS generation and to induce apoptosis in colon and hepatocellular cancer cells [9, 12], and may induce apoptosis and inhibit migration of ovarian SKOV3 cells by inhibiting the phosphorylation of tyrosine protein kinase Src (Src) and focal adhesion kinase (FAK) [20].

Our results show that SHK significantly inhibited type 2 ovarian cancer cell proliferation, migration, and invasion in vitro. We found that treatment with SHK resulted in the death of type 2 ovarian cancer cells via the activation of the apoptosis signaling pathway. It decreased type 2 ovarian CSC gene expression and also inhibited the tumorigenicity of CSCs of KURAMOCHI cells via induced apoptosis in NOD-SCID mice. These findings suggest that SHK may be useful in type 2 ovarian cancer therapy. Thus, we suggest that SHK could be considered as a possible therapeutic candidate for the clinical treatment of ovarian cancer.

Acknowledgements

We thank the Ministry of Science and Technology, Taiwan, ROC, the Buddhist Tzu Chi General Hospital, and Buddhist Tzu Chi Medical Foundation for the funding. This research was funded by the Ministry of Science and Technology, Taiwan, ROC (MOST 104-2314-B-303-MY3), the Buddhist Tzu Chi General Hospital (TCRD 107-44), and Buddhist Tzu Chi Medical Foundation (TCMF-EP-108-02).

Disclosure of conflict of interest

None.

Abbreviations

SHK, Shikonin; HGSC, High-Grade Serous Carcinomas; RIPK1, Receptor-Interacting Protein 1; EOC, Epithelial Ovarian Cancer; XIAP, X-Linked Inhibitor Of Apoptosis Protein; TUNEL, Terminal Deoxynucleotidyl Transferase Dutp Nick End Labeling; ALDH, Acetaldehyde Dehydrogenase; CSC, Cancer Stem Cell; FAK, Focal Adhesion Kinase.

Address correspondence to: Dah-Ching Ding, Department of Obstetrics and Gynecology, Hualien Tzu Chi Hospital, Buddhist Tzu Chi Medical Foundation, Tzu Chi University, Hualien 970, Taiwan; Institute of Medical Sciences, Tzu Chi University, Hualien 970, Taiwan. Tel: +886-3-8561825-15739; Fax: +886-3-8577161; E-mail: dah1003@yahoo.com.tw; Tomor Harnod, Department of Neurosurgery, Hualien Tzu Chi Hospital, Buddhist Tzu Chi Medical Foundation, Tzu Chi University, Hualien 970, Taiwan. Tel: +886-3-8561825-19000; E-mail: tomorha@yahoo.com.tw

References

[1] Karst AM and Drapkin R. The new face of ovarian cancer modeling: better prospects for detection and treatment. F1000 Med Rep 2011; 3: 22.

[2] Hong MK, Chu TY and Ding DC. The fallopian tube is the culprit and an accomplice in type II ovarian cancer: a review. Tzu Chi Med J 2013; 25: 203-205.

[3] Kurman RJ and Shih IeM. Pathogenesis of ovarian cancer: lessons from morphology and molecular biology and their clinical implications. Int J Gynecol Pathol 2008; 27: 151-160.

[4] Kurman RJ and Shih IeM. The origin and pathogenesis of epithelial ovarian cancer: a proposed unifying theory. Am J Surg Pathol 2010; 34: 433-443.

[5] Fathalla MF. Incessant ovulation-a factor in ovarian neoplasia? Lancet 1971; 2: 163.

[6] Oronsky B, Ray CM, Spira AI, Trepel JB, Carter CA and Cottrill HM. A brief review of the management of platinum-resistant-platinum-refractory ovarian cancer. Med Oncol 2017; 34: 103.

[7] Lu L, Qin A, Huang H, Zhou P, Zhang C, Liu N, Li S, Wen G, Zhang C, Dong W, Wang X, Dou QP and Liu J. Shikonin extracted from medicinal Chinese herbs exerts anti-inflammatory effect via proteasome inhibition. Eur J Pharmacol 2011; 658: 242-247.

[8] Chen X, Yang L, Oppenheim JJ and Howard MZ. Cellular pharmacology studies of shikonin derivatives. Phytother Res 2002; 16: 199-209.

[9] Gong K and Li W. Shikonin, a Chinese plant-derived naphthoquinone, induces apoptosis in

hepatocellular carcinoma cells through reactive oxygen species: a potential new treatment for hepatocellular carcinoma. Free Radic Biol Med 2011; 51: 2259-2271.
[10] Zhao Q, Assimopoulou AN, Klauck SM, Damianakos H, Chinou I, Kretschmer N, Rios JL, Papageorgiou VP, Bauer R and Efferth T. Inhibition of c-MYC with involvement of ERK/JNK/MAPK and AKT pathways as a novel mechanism for shikonin and its derivatives in killing leukemia cells. Oncotarget 2015; 6: 38934-38951.
[11] Yang YY, He HQ, Cui JH, Nie YJ, Wu YX, Wang R, Wang G, Zheng JN, Ye RD, Wu Q, Li SS and Qian F. Shikonin derivative DMAKO-05 inhibits akt signal activation and melanoma proliferation. Chem Biol Drug Des 2016; 87: 895-904.
[12] He G, He G, Zhou R, Pi Z, Zhu T, Jiang L and Xie Y. Enhancement of cisplatin-induced colon cancer cells apoptosis by shikonin, a natural inducer of ROS in vitro and in vivo. Biochem Biophys Res Commun 2016; 469: 1075-1082.
[13] Zhang Y, Qian RQ and Li PP. Shikonin, an ingredient of Lithospermum erythrorhizon, downregulates the expression of steroid sulfatase genes in breast cancer cells. Cancer Lett 2009; 284: 47-54.
[14] Fu Z, Deng B, Liao Y, Shan L, Yin F, Wang Z, Zeng H, Zuo D, Hua Y and Cai Z. The anti-tumor effect of shikonin on osteosarcoma by inducing RIP1 and RIP3 dependent necroptosis. BMC Cancer 2013; 13: 580.
[15] Lui WO, Pourmand N, Patterson BK and Fire A. Patterns of known and novel small RNAs in human cervical cancer. Cancer Res 2007; 67: 6031-6043.
[16] Que K, Tong Y, Que G, Li L, Lin H, Huang S, Wang R and Tang L. Downregulation of miR-874-3p promotes chemotherapeutic resistance in colorectal cancer via inactivation of the Hippo signaling pathway. Oncol Rep 2017; 38: 3376-3386.
[17] Xia B, Lin M, Dong W, Chen H, Li B, Zhang X, Hou Y and Lou G. Upregulation of miR-874-3p and miR-874-5p inhibits epithelial ovarian cancer malignancy via SIK2. J Biochem Mol Toxicol 2018; 32: e22168.
[18] Wang Y, Yan C, Qi J, Liu C, Yu J and Wang H. MiR-874-3p mitigates cisplatin resistance through modulating NF-kappaB/inhibitor of apoptosis protein signaling pathway in epithelial ovarian cancer cells. Mol Cell Biochem 2022; 477: 307-317.
[19] Matthaiou EI, Barar J, Sandaltzopoulos R, Li C, Coukos G and Omidi Y. Shikonin-loaded antibody-armed nanoparticles for targeted therapy of ovarian cancer. Int J Nanomedicine 2014; 9: 1855-1870.
[20] Hao Z, Qian J and Yang J. Shikonin induces apoptosis and inhibits migration of ovarian carcinoma cells by inhibiting the phosphorylation of Src and FAK. Oncol Lett 2015; 9: 629-633.
[21] Domcke S, Sinha R, Levine DA, Sander C and Schultz N. Evaluating cell lines as tumour models by comparison of genomic profiles. Nat Commun 2013; 4: 2126.
[22] Parker RJ, Eastman A, Bostick-Bruton F and Reed E. Acquired cisplatin resistance in human ovarian cancer cells is associated with enhanced repair of cisplatin-DNA lesions and reduced drug accumulation. J Clin Invest 1991; 87: 772-777.
[23] Sebaugh JL. Guidelines for accurate EC50/IC50 estimation. Pharm Stat 2011; 10: 128-134.
[24] Chang YH, Liu HW, Chu TY, Wen YT, Tsai RK and Ding DC. Cisplatin-impaired adipogenic differentiation of adipose mesenchymal stem cells[1]. Cell Transplant 2017; 26: 1077-1087.
[25] Lin CC, Chen KB, Tsai CH, Tsai FJ, Huang CY, Tang CH, Yang JS, Hsu YM, Peng SF and Chung JG. Casticin inhibits human prostate cancer DU 145 cell migration and invasion via Ras/Akt/NF-kappaB signaling pathways. J Food Biochem 2019; 43: e12902.
[26] Livak KJ and Schmittgen TD. Analysis of relative gene expression data using real-time quantitative PCR and the 2(-Delta Delta C(T)) Method. Methods 2001; 25: 402-408.
[27] Liu SP, Shibu MA, Tsai FJ, Hsu YM, Tsai CH, Chung JG, Yang JS, Tang CH, Wang S, Li Q and Huang CY. Tetramethylpyrazine reverses high-glucose induced hypoxic effects by negatively regulating HIF-1alpha induced BNIP3 expression to ameliorate H9c2 cardiomyoblast apoptosis. Nutr Metab (Lond) 2020; 17: 12.
[28] Zuberi M, Khan I, Mir R, Gandhi G, Ray PC and Saxena A. Utility of serum miR-125b as a diagnostic and prognostic indicator and its alliance with a panel of tumor suppressor genes in epithelial ovarian cancer. PLoS One 2016; 11: e0153902.
[29] Wang Q, Yang G, Jiang Y, Luo M, Li C, Zhao Y, Xie Y, Song K and Zhou J. XB130, regulated by miR-203, miR-219, and miR-4782-3p, mediates the proliferation and metastasis of non-small-cell lung cancer cells. Mol Carcinog 2020; 59: 557-568.
[30] Medeiros F, Muto MG, Lee Y, Elvin JA, Callahan MJ, Feltmate C, Garber JE, Cramer DW and Crum CP. The tubal fimbria is a preferred site for early adenocarcinoma in women with familial ovarian cancer syndrome. Am J Surg Pathol 2006; 30: 230-236.
[31] Lee Y, Miron A, Drapkin R, Nucci MR, Medeiros F, Saleemuddin A, Garber J, Birch C, Mou H, Gordon RW, Cramer DW, McKeon FD and Crum CP. A candidate precursor to serous carcinoma

that originates in the distal fallopian tube. J Pathol 2007; 211: 26-35.
[32] du Bois A, Luck HJ, Meier W, Adams HP, Mobus V, Costa S, Bauknecht T, Richter B, Warm M, Schroder W, Olbricht S, Nitz U, Jackisch C, Emons G, Wagner U, Kuhn W and Pfisterer J; Arbeitsgemeinschaft Gynakologische Onkologie Ovarian Cancer Study Group. A randomized clinical trial of cisplatin/paclitaxel versus carboplatin/paclitaxel as first-line treatment of ovarian cancer. J Natl Cancer Inst 2003; 95: 1320-1329.
[33] Cannistra SA. Cancer of the ovary. N Engl J Med 2004; 351: 2519-2529.
[34] Poveda A, Floquet A, Ledermann JA, Asher R, Penson RT, Oza AM, Korach J, Huzarski T, Pignata S, Friedlander M, Baldoni A, Park-Simon TW, Tamura K, Sonke GS, Lisyanskaya A, Kim JH, Filho EA, Milenkova T, Lowe ES, Rowe P, Vergote I and Pujade-Lauraine E; SOLO2/ENGOT-Ov21 investigators. Olaparib tablets as maintenance therapy in patients with platinum-sensitive relapsed ovarian cancer and a BRCA1/2 mutation (SOLO2/ENGOT-Ov21): a final analysis of a double-blind, randomised, placebo-controlled, phase 3 trial. Lancet Oncol 2021; 22: 620-631.
[35] Weroha SJ, Becker MA, Enderica-Gonzalez S, Harrington SC, Oberg AL, Maurer MJ, Perkins SE, AlHilli M, Butler KA, McKinstry S, Fink S, Jenkins RB, Hou X, Kalli KR, Goodman KM, Sarkaria JN, Karlan BY, Kumar A, Kaufmann SH, Hartmann LC and Haluska P. Tumorgrafts as in vivo surrogates for women with ovarian cancer. Clin Cancer Res 2014; 20: 1288-1297.
[36] Scott CL, Becker MA, Haluska P and Samimi G. Patient-derived xenograft models to improve targeted therapy in epithelial ovarian cancer treatment. Front Oncol 2013; 3: 295.
[37] Thakur R, Trivedi R, Rastogi N, Singh M and Mishra DP. Inhibition of STAT3, FAK and Src mediated signaling reduces cancer stem cell load, tumorigenic potential and metastasis in breast cancer. Sci Rep 2015; 5: 10194.
[38] Kenda Suster N and Virant-Klun I. Presence and role of stem cells in ovarian cancer. World J Stem Cells 2019; 11: 383-397.
[39] Zhong JX, Zhou L, Li Z, Wang Y and Gui JF. Zebrafish Noxa promotes mitosis in early embryonic development and regulates apoptosis in subsequent embryogenesis. Cell Death Differ 2014; 21: 1013-1024.
[40] Nainu F, Tanaka Y, Shiratsuchi A and Nakanishi Y. Protection of insects against viral infection by apoptosis-dependent phagocytosis. J Immunol 2015; 195: 5696-5706.
[41] Hsin IF, Montano E and Seki E. Finding a new role for NEMO: A key player in preventing hepatocyte apoptosis and liver tumorigenesis by inhibiting RIPK1. Hepatology 2016; 64: 295-297.
[42] Marhaba R, Freyschmidt-Paul P and Zoller M. In vivo CD44-CD49d complex formation in autoimmune disease has consequences on T cell activation and apoptosis resistance. Eur J Immunol 2006; 36: 3017-3032.
[43] Wu SH, Hang LW, Yang JS, Chen HY, Lin HY, Chiang JH, Lu CC, Yang JL, Lai TY, Ko YC and Chung JG. Curcumin induces apoptosis in human non-small cell lung cancer NCI-H460 cells through ER stress and caspase cascade- and mitochondria-dependent pathways. Anticancer Res 2010; 30: 2125-2133.
[44] Das DS, Ray A, Das A, Song Y, Tian Z, Oronsky B, Richardson P, Scicinski J, Chauhan D and Anderson KC. A novel hypoxia-selective epigenetic agent RRx-001 triggers apoptosis and overcomes drug resistance in multiple myeloma cells. Leukemia 2016; 30: 2187-2197.
[45] Renschler MF. The emerging role of reactive oxygen species in cancer therapy. Eur J Cancer 2004; 40: 1934-1940.

Table S1. The primer sequences of the genes

Primer Name	Sequence	Product (bp)
Nanog-F	CAG AAG GCC TCA GCA CCT AC	111
Nanog-R	ATT GTT CCA GGT CTG GTT GC	
Oct4-F	CAG TGC CCG AAA CCC ACA C	161
Oct4-R	GGA GAC CCA GCA GCC TCA AA	
Sox2-F	GGG AAA TGG GAG GGG TGC AAA AGA GG	151
Sox2-R	TTG CGT GAG TGT GGA TGG GAT TGG TG	
c-Myc-F	AAA CAC AAA CTT GAA CAG CTA C	188
c-Myc-R	ATT TGA GGC AGT TTA CAT TAT GG	
ALDH1-F	TTG GAA TTT CCC GTT GGT TA	182
ALDH1-R	CTG TAG GCC CAT AAC CAG GA	
miR-874-3p-F	GAA CTC CAC TGT AGC AGA GAT GGT	
miR-874-3p-R	CAT TTT TTC CAC TCC TCT TCT CTC	

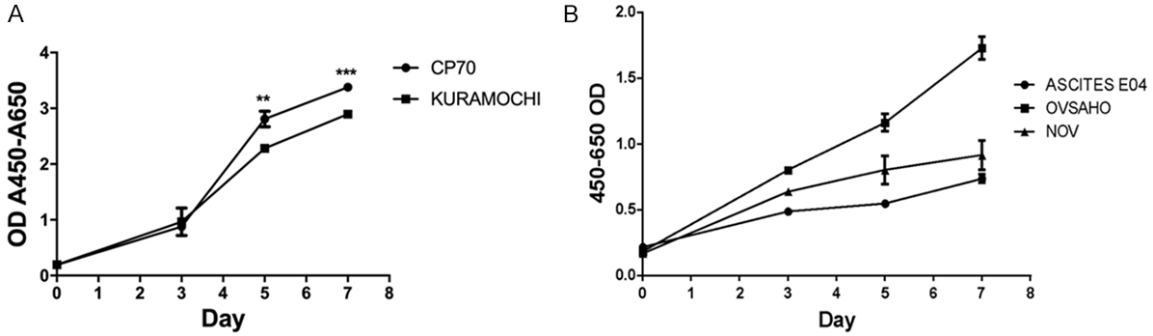

Figure S1. The proliferation curve on various ovarian cancer cells. The KURAMOCHI and CP70 cells exhibited a normal growth curve. But OVSAHO and E04 cells grew at a slower rate than the previous two cells.

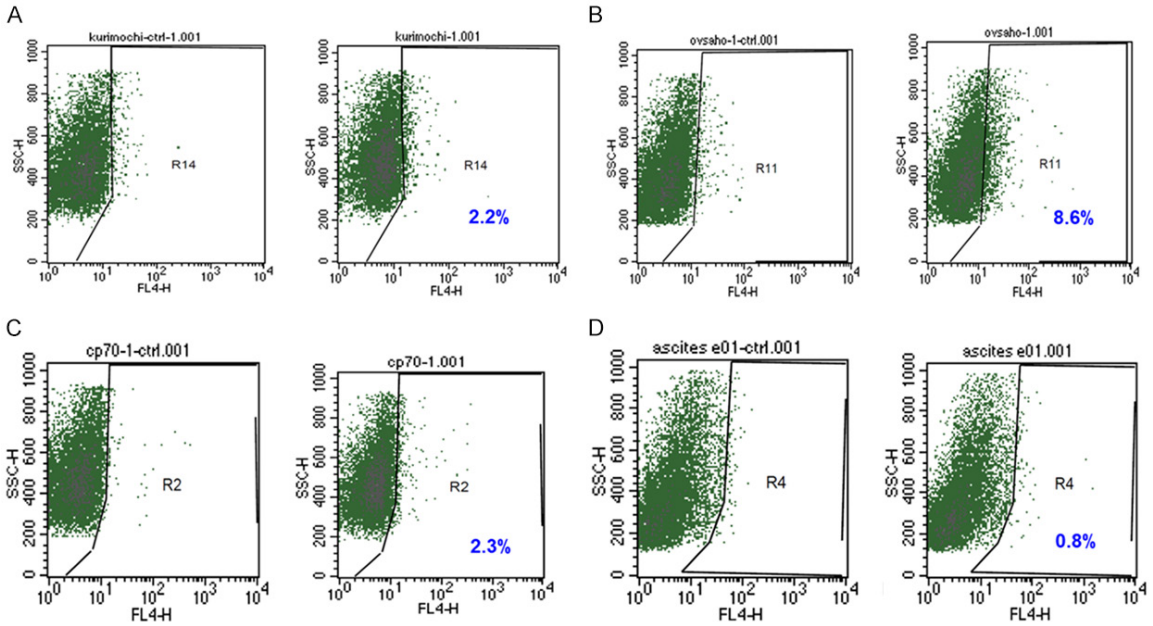

Figure S2. The expressions of cancer stem cell marker ALDH in various ovarian cancer cells. KURAMOCHI, OVSAHO, CP70, and E04 cells were measured through flow cytometry using the Aldefluror assay. Values mentioned along with the dot plots indicate the percentage of ALDH+ population.